Anal. Bioanal. Electrochem., Vol. 17, No. 8, 2025, 646-661
https://www.doi.org/10.22034/abec.2025.733508

Analytical & Bioanalytical Electrochemistry

www.abechem.com

Full Paper

Beyond Randles-Sevcik Formalism: Towards Understanding Peak Currents of Nernstian Redox Systems in Square-Wave Voltammetry

Milkica Janeva, Pavlinka Kokoskarova, and Rubin Gulaboski*

Faculty of Medical Sciences, Goce Delcev University, Stip, Macedonia

*Corresponding Author, Tel.: +38975331078
E-Mail: rubin.gulaboski@ugd.edu.mk

Received: 7 July 2025 / Received in revised form: 16 September 2025 / Accepted: 28 September 2025 / Published online: 31 December 2025

Abstract- In redox systems that obey the Nernst equation, where the surface and bulk concentrations remain in equilibrium during the potential sweep, the Randles-Sevcik equation is seen as a standard tool in both fundamental and applied linear scan voltammetry. As the Randles-Sevcik equation is seen as a key theoretical framework for interpreting voltammetric behavior in electrochemically reversible and diffusion-controlled redox systems considered under conditions of linear scan voltammetry, this foundational relationship becomes inapplicable when extended to pulse voltammetric techniques. Pulse voltammetric techniques differ fundamentally from linear scan voltammetric methods in both potential modulation and in current measurement protocols. The form of applied bias in pulse voltammetric techniques leads to conditions in which each applied pulse disrupts the diffusion profile of redox species of interest. Repeated disruption and compression of diffusion profiles in pulse voltammetric techniques introduce significant complexity into the current-potential behavior of redox species, thereby precluding the direct application of the Randles-Sevcik formalism. This study presents some basic theoretical insights into the limitations of applying Randles–Sevcik-type equations to square-wave voltammetry. In addition, a unifying parameter has been identified that governs the peak current response in square-wave voltammetry, which integrates the effects of potential step, frequency, square-wave amplitude, and temperature. At constant magnitude of the diffusion coefficient, this critical parameter is defined as $\chi = constant \cdot (F/RT)\cdot[E_{sw}/(dE\cdot f)]^{1/2}$ and it is seen as a foundation for developing more comprehensive models and analytical expressions describing peak current dependencies under square-wave voltammetric conditions.

Keywords- Randles-Sevcik equation; Square-wave voltammetry; Square-wave amplitude; peak currents in pulse techniques; Concentration gradients

1. INTRODUCTION

Voltammetric methods are widely recognized as some of the fastest, most cost-effective, and most efficient tools designed for investigating the mechanistic, kinetic, and thermodynamic aspects of various redox systems [1-3]. Owing mainly to its simplicity, sensitivity, and robust diagnostic capabilities, the cyclic voltammetry (CV) stands out as one of the most extensively employed among the other electrochemical techniques [3]. Major advantages of CV arise from its distinctive operational protocols and the easiness in interpretability the resulting voltammetric outputs. The fundamental principles of cyclic voltammetric theory provide a clear and systematic basis for interpreting complex electrochemical mechanisms, while also offering a very practical framework for kinetic measurements and analytical applications. Among the foundational concepts in the analysis of data obtained by conventional linear scan cyclic voltammetry stays the so-called "Randles-Sevcik equation" [2-6]. As it quantitatively relates the magnitudes of peak currents to the key parameters governing diffusion-controlled reversible electrode reactions, this equation represents a cornerstone in mechanistic investigations, analytical determinations, and in evaluation of diffusion coefficients of redox species of interest. The Randles-Sevcik equation is particularly applicable in linear scan voltammetry for electrochemical systems exhibiting Nernstian behavior, implying that the electrode reaction remains reversible and maintains near-equilibrium conditions throughout entire potential sweep. The Randles-Sevcik equation establishes a simple relationship between the magnitude of measured peak current (I_p) and several key parameters, including the analyte's of interest bulk concentration, applied scan rate, temperature, and the diffusion coefficients of redox active forms [4-7]. Generally speaking, this equation makes a direct correlation between the magnitude of the measured voltammetric peak currents and the mass transport properties of electroactive redox species that are dissolved in solution. At 25ºC (298 K), for electrochemically reversible electrode reaction in which electrons are exchanged in one-step, this equation can be written in following well-known form [2-4,7]:

$$I_p = 2.69 \times 10^5 \, n^{3/2} \, D^{1/2} \, A \, c^* v^{1/2} \quad (1)$$

In equation (1) "*n*" stays for the number of electrons transferred, "*A*" stays for the active area of working electrode, "*D*" is the diffusion coefficient of the molecules/ions of redox active species of interest, "*c**" is the bulk molar concentration of the redox analyte of interest, while "*v*" is the applied scan rate. The square-root dependence of the peak current on applied scan rate (*v*) and on the diffusion coefficient makes this equation a basis for determining diffusion coefficients of electroactive species of interest, but it is also suitable for assessing the electrochemical reversibility of electron transfer processes. Its relevance extends to studies of biological redox centers of water-soluble enzymes, water-soluble coordination complexes, battery materials, in biosensors design, and many more [1-4].

Although the Randles-Sevcik equation serves as a fundamental analytical tool in voltammetric techniques exhibiting a linear sweep of the applied potential, its applicability breaks down when extended to pulse voltammetric techniques such as differential pulse voltammetry (DPV) and square-wave voltammetry (SWV). Pulse voltammetric techniques employ fundamentally different operating protocols, particularly in the potential modulations, and in the manner the current is sampled in each of the applied pulses [2,8-10]. These specific features, in turn, lead to significant deviations from the conditions under which the Randles-Sevcik equation holds. As it is already well elaborated elsewhere [2,8-10], in the pulse voltammetric technique, current is not measured continuously. Instead, it is sampled at specific time intervals, commonly at the end of each applied potential pulse. The aim of such a current-measuring protocol in pulse voltammetric techniques is to efficiently discriminate the capacitive (non-Faradaic) current [2,9,10]. Upon application of each potential pulse in pulse voltammetric techniques, perturbations of the electrochemical double layer induce distortions of the diffusional profile of the redox species of interest [10]. As a result, the diffusion layer does not evolve in a continuous, linear fashion, as assumed in linear scan voltammetry. Instead, the diffusion profile is periodically disrupted and re-created with each applied potential pulse. Such a repeated perturbation of the diffusion layer profile in pulse voltammetric techniques introduces a level of complexity that renders the direct application of the Randles-Sevcik formalism. Notably, in pulse voltammetric techniques, the peak current becomes a complex function of all signal parameters associated with the applied potential excitation waveform. In SWV, for example, the measured current depends on all parameters of the applied potential signal, i.e., the SW frequency, the SW pulse amplitude, and the potential step of the applied square-wave pulses [9]. In the voltammetric experiments, these parameters significantly affect the effective thickness of the diffusion layer, often resulting in complex voltammetric responses in which peak currents exhibit a nonlinear dependence on the applied signal parameters [9, 10]. Consequently, the interpretation of peak current dependencies in pulse voltammetric techniques requires alternative models that explicitly account for the transient nature of mass transport and the dynamic reconfiguration of the interfacial region during each applied potential pulse. The non-steady-state conditions, altered diffusion dynamics, and distinct measurement protocols inherent to these methods necessitate a fundamentally different analytical framework for accurate data interpretation, which has not been developed so far. Thus, while the Randles-Sevcik equation remains a cornerstone in linear scan voltammetric analysis, its assumptions are not completely met in pulse voltammetric techniques. In this study, we present a set of theoretical results aimed at elucidating the limitations of applying Randles-Sevcik-like equations to describe the peak current dependences in square-wave voltammetry. Furthermore, we identify and discuss the key parameters that govern the magnitudes of peak current responses and influence the apparent reversibility of redox processes under square-wave voltammetric conditions. The analyses presented in this work

provide a foundational basis for the development of more comprehensive theoretical models, ultimately enabling the formulation of analytical expressions describing peak current dependencies in square-wave voltammetry.

2. MATHEMATICAL MODEL

In this study, a theoretical model of a "Nernstian" (electrochemically reversible), diffusion-controlled electrode reaction of the type $Ox + 1e^- \rightleftharpoons Red$ was investigated under conditions of square-wave voltammetry. The simulation protocol employed follows the methodology outlined in [9]. Square-wave voltammograms were calculated by using the MATHCAD commercial software package, implementing the algorithm described in more detail in [11].

3. RESULTS AND DISCUSSION

3.1. The effect of square-wave frequency and the "effective scan rate" in square-wave voltammetry

Theoretical square-wave voltammograms of a simple one-electron, diffusion-controlled reversible Nernstian electrode reaction exhibit almost symmetrical forward and backward current peaks, centered around the formal potential (E°) (Figure 1a). As elaborated in [9], the features of theoretical SW voltammograms are primarily governed by the square-wave amplitude (E_{sw})**,** step potential (dE)**,** frequency (f)**,** temperature (T), and the diffusion coefficient (D)**** of the electroactive species. The peak shape and intensity of both SW peaks are highly sensitive to these factors. Under constant temperature, step potential, and amplitude, the dimensionless peak current**s** are inversely proportional to the square root of the product of frequency and diffusion coefficient. For a given magnitude of D, the parameter $(D \times f)^{0.5}$ reflects the reduced diffusion time at higher frequencies, which limits the development of concentration gradients and thus lowers the peak currents [9]. Consequently, increasing frequency commonly results in diminished current responses of theoretical dimensionless SW peak currents. Importantly, for an ideal Nernstian redox system, the peak-to-peak separation between forward and backward currents remains constant, even at very high frequencies, while the peak current ratio (oxidation/reduction) remains unity across all frequencies applied. These criteria are commonly used to define the term "electrochemical reversibility" under the conditions of square-wave voltammetry [9]. All these features are nicely demonstrated in Figure 1a, where the behavior of forward and backward voltammetric profiles is evaluated as a function of applied frequency, while Figure 1b showcases the forward peak currents plotted *vs*. $f^{0.5}$. In square-wave voltammetry, however, instead of interpreting the results in light of the effect of frequency, one often (especially by commercial potentiostats producers) explores the term "effective scan rate" [12].

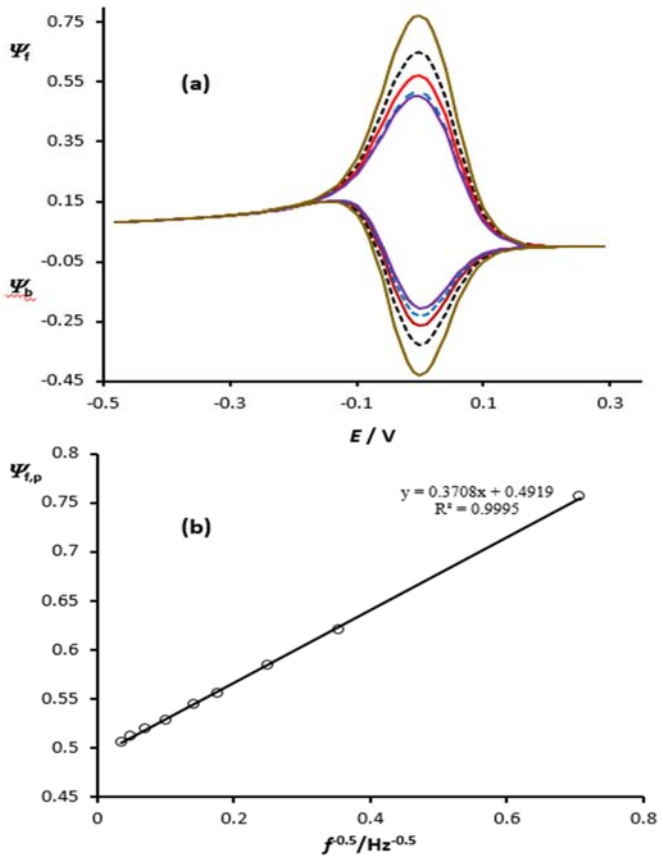

Figure 1. (a) Forward and backward components of the square-wave voltammograms plotted as a function of the applied square-wave frequencies. **(b)** Graph of the dependence of the forward peak current as a function of the inverse square root of the applied frequencies. In all simulations, the initial potential was fixed at + 0.3 V, while the other calculation parameters were: temperature T = 298.15 K, potential step dE = 4 mV, and square-wave amplitude E_{sw} = 50 mV

The effective scan rate in SWV is commonly defined as v = dE x f. This parameter is commonly seen as an indicator that shows how rapidly the potential is swept through the redox region upon applying a single potential SW pulse. In general context, the effective scan rate is crucial parameter used to assess the balance between kinetics of electron transfer and the rate of mass transport. Understanding this parameter helps in interpreting how experimental conditions affect peak shapes, peak position, and the peak current magnitude. Shown in Figure 2 is a series of voltammetric patterns, calculated at identical "effective scan rates" that are obtained for different combinations of dE and f. The potential step, defined as the increment between successive potential pulses in square-wave voltammetry (SWV) [9], plays a critical role in shaping the resulting voltammetric response. As the potential step increases, the calculated voltammogram covers a broader potential range in a shorter number of pulses, thus

leading to broader and more pronounced peak features. This enlargement of the peaks at higher potential step magnitudes arises due to the greater driving force for electron transfer, which enhances the overall current response, while reducing the same time resolution of current-potential response by merging closely spaced redox events. Note that in all patterns in Figure 2, the effective scan rate is the same, but this parameter is achieved by different combinations of the magnitude of the potential step and that of the applied square-wave frequency. Notably, the effective scan rate does not cause a shift of the positions of both peaks, indicating that peak potentials are predominantly governed by the thermodynamics of the redox process. However, the ratio between the forward and backward peak currents shows a subtle dependence on the effective scan rate, despite the fact that the nominal scan rate remains constant across all voltammetric patterns displayed in Figure 2. This behavior likely arises from some asymmetries in mass transport dynamics that become more pronounced under faster perturbation conditions. The behavior of square-wave voltammograms displayed in Figure 2 underscores the importance of potential step and the SW frequency (i.e. the effective scan rate) in terms of better quantitative interpretation of peak-current dependences in SWV.

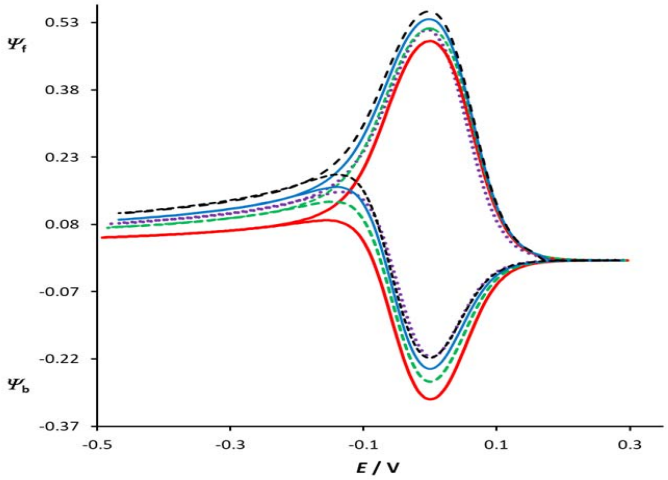

Figure 2. Forward and backward current components of square-wave voltammograms simulated at an "effective" scan rate of 200 mV/s, achieved by various combinations of potential step (dE) and frequency (f): dE = 2 mV, f = 100 Hz (……); dE = 4 mV, f = 50 Hz (——); dE = 5 mV, f = 40 Hz (------); dE = 8 mV, f = 25 Hz (—); and dE = 10 mV, f = 20 Hz (------). All other simulation parameters were identical to those reported in Figure 1.

3.2. Effect of the square-wave amplitude

It is already reported [9,10,13,14], that the application of each potential pulse in pulse voltammetric techniques perturbs the electrochemical double thereby altering the concentration

gradients of the redox species within the diffusion layer [15-17]. Unlike linear scan voltammetry, where the diffusion layer evolves gradually and predictably [2-4], SWV imposes periodic interruptions to this development [9]. Application of each successive potential SW pulse induces a transient reorganization of the diffusion profile, thus preventing a steady-state or linear progression within. These repeated disturbances create complex and time-dependent concentration profiles of redox-active species of interest that must be considered when interpreting the current-potential responses in SWV [9,11]. It is particularly important to note that the amplitude of the square-wave pulses plays a critical role in modulating this complexity, as it governs the interplay between the thermodynamic driving force and the extent of diffusion-layer evolution [18]. Therefore, it is of utmost importance to this study to understand the effect of square-wave amplitude on the development of square-wave voltammetric patterns. Shown in Figure 3 is a series of 3-D voltammetric patterns (forward and backward current components), calculated at different SW amplitudes. The absence of a backward peak in theoretical voltammograms calculated at low square-wave amplitudes (at E_{sw} of 10 mV or lower) is due to the insufficient overpotential to significantly drive the reverse (oxidation) reaction within the short pulse time.

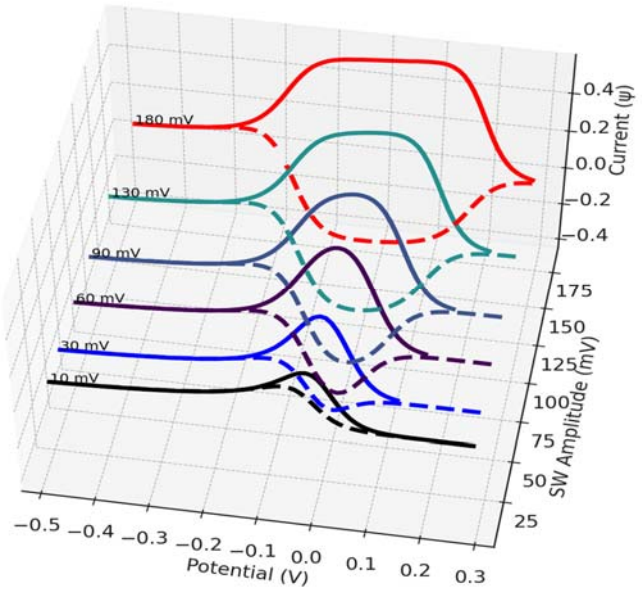

Figure 3. Forward and backward 3D current profiles of square-wave voltammograms simulated at varying square-wave amplitudes. A fixed frequency of 50 Hz was applied for all calculations, while all other simulation parameters were identical to those reported in Figure 1.

At low amplitudes, the potential excursions are close to the formal potential (E^{e}), where the system remains near equilibrium. In such a scenario, it is more likely that the same electrode transformation that takes place in the forward scan also happens in the backward scan. This

results in minimal driving force for the backward electron transfer during the reverse pulse, leading to small backward currents and the absence of a distinct backward peak. Essentially, the redox reaction does not proceed far enough in either direction to generate a noticeable reverse signal. So, when square-wave amplitudes exceed approximately 30 mV**,** the backward current components of the square-wave voltammograms begin to develop noticeably. This is because the increased amplitude provides a suitable overpotential**,** which drives the redox reaction further enough from equilibrium during each applied pulse. At these overpotentials, the electron transfer becomes more extensive, and sufficient time exists within each potential pulse for a concentration gradient to begin forming in the diffusion layer. This gradient enables both oxidation and reduction processes to generate measurable currents in forward and backward directions, leading to the appearance of distinct backward peaks in the voltammogram. On the other hand, at rather high square-wave amplitudes (e.g., at $E_{sw} > 90$ mV), both forward and backward current components tend to form broad plateaus rather than sharp or normally developed peaks. This occurs because the large potential excursions (e.g., ± 100 mV or higher) drive the system far from the equilibrium potential. The fast potential jumps cause rapid and nearly complete oxidation and reduction during each half-cycle of the square wave, so the surface concentration in the diffusional layer of the electroactive species is quickly depleted. As a result, the current becomes diffusion-limited almost immediately, and there is no time to re-establish a concentration gradient of redox-active species between applied pulses. Therefore, the current response at large SW amplitudes gets plateau-shaped features rather than the common peak-shaped. Any further increases in pulse amplitude do not contribute to the increase of peak currents. This behavior contrasts with the linear or quasi-linear increase in peak current observed at moderate amplitudes (e.g., 30–90 mV), where diffusion still governs the response. This plateauing of peak current at large square-wave amplitudes highlights one of the key limitations in applying Randles–Sevcik-type relationships to square-wave voltammetry. Since the current response under these conditions is no longer governed by linear diffusion but is instead constrained by the inability of concentration gradients to form within the short pulse duration, the major assumptions underlying the Randles–Sevcik equation break down.

3.3. Effect of the temperature on the features of calculated square-wave voltammograms

The effect of the temperature on the behavior of theoretical square-wave voltammograms of surface-active redox systems obeying Butler-Volmer formalism is elaborated in more detail elsewhere [19]. In voltammetric simulations, temperature is a parameter incorporated within the potential-dependent term of the Nernst equation, thereby influencing all features of the calculated square-wave voltammograms.

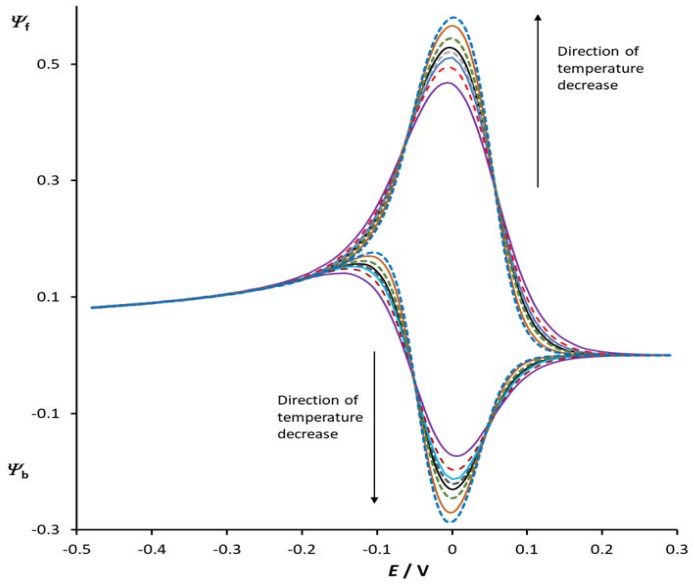

Figure 4. Evolution of forward and backward current components of square-wave voltammograms as a function of temperature. Simulations were performed at temperatures T = 203, 223, 253, 274, 286, 298, 323, and 363 K, with the curves corresponding to increasing temperatures showing progressively lower current intensities. The simulation conditions included a frequency of 50 Hz, a square-wave amplitude of 60 mV, and a potential step of 10 mV.

As shown in Figure 4, decreasing the temperature leads to a notable increase in the peak currents of both oxidation and reduction processes. Simultaneously, the voltammetric peaks become sharper and more narrowly defined, the peak-to-peak separation diminishes, while the overall symmetry between the forward and backward peaks becomes more pronounced. The development of the net SW peaks as a function of the temperature, and the dependence between the net SW peaks and the inverse temperature are displayed in Figure 5a and 5b, respectively. Notably, the magnitudes of net SW peaks follow a linear dependence as a function of inverse temperature in the region of applied temperatures. The influence of temperature on the development of square-wave voltammograms becomes particularly evident when analyzing voltammograms calculated at small pulse amplitudes. Shown in Figure 6 is a series of 3D voltammograms calculated at SW amplitude of 25 mV, where the effect of temperature is displayed. The 3D visualization of square-wave voltammograms recorded at an amplitude of 25 mV clearly demonstrates the significant influence of temperature on the electrochemical behavior of the considered diffusion-controlled Nernstian electrode mechanism. As the temperature decreases, a marked increase in the peak intensities is observed for both the forward and backward currents. At lower temperatures, the backward currents become more

pronounced and start to mirror their forward counterparts more closely, thus indicating an improvement in the overall apparent electrochemical reversibility.

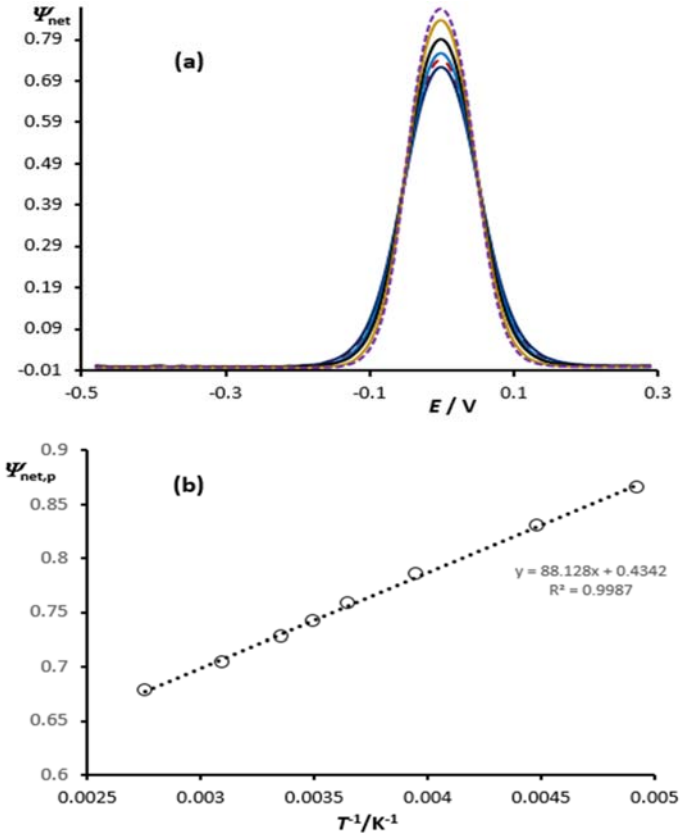

Figure 5. (**a**) Evolution of calculated net square-wave voltammograms as a function of temperature, and (**b**) the corresponding dependence of net peak currents on the inverse of thermodynamic temperature (1/*T*). All simulation parameters were identical to those used in Figure 4.

The symmetry between the forward and backward peaks becomes more evident, especially at the lowest temperatures examined, implying that temperature exerts a critical role in modulating both the intensity and reversibility of square-wave voltammetric responses. The behavior of calculated voltammetric patterns presented in Figures 4, 5, and 6 arises from the temperature-dependent nature of the thermodynamic term governing concentration gradients near the electrode surface. At lower temperatures, the distribution of redox states around the formal potential narrows, which in turn leads to more abrupt changes in current near the redox potential. However, it is important to note that in real experimental conditions, the diffusion coefficients of electroactive species are also temperature-dependent parameters, typically decreasing by lowering the temperature [2,3], which introduces an additional level of complexity in experimental scenarios. As a result, experimentally observed peak currents may

not follow the same trends as those predicted by idealized simulations, where diffusion coefficients are held constant (as has been done in Figures 4 to 6 in this work).

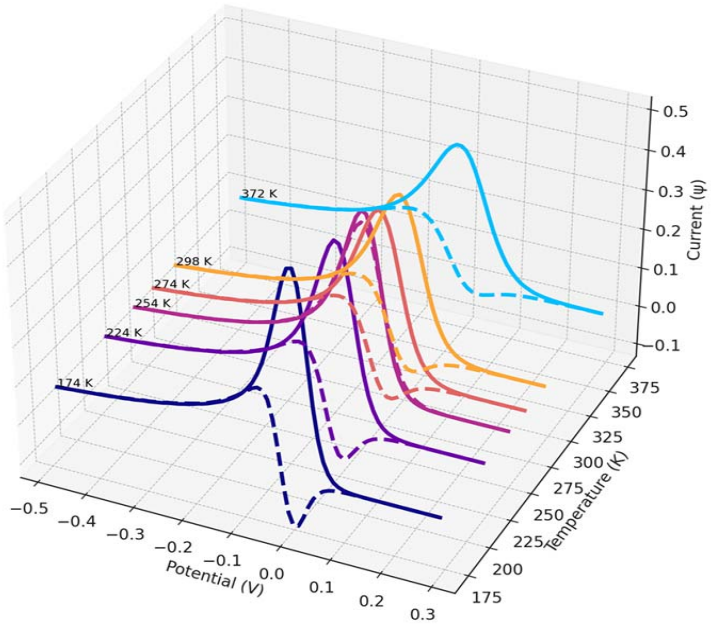

Figure 6. Three-dimensional profiles illustrating the effect of temperature on the evolution of forward and backward current components of square-wave voltammograms, simulated at a low square-wave amplitude of 25 mV. All other simulation parameters were identical to those described in Figure 4.

3.4. If the Randles-Sevcik formalism is not applicable to SWV, is there any parameter that governs the peak current magnitudes in square-wave voltammetry?

As shown in previous segments of this work, the Randles–Sevcik equation, traditionally used to describe peak currents in linear scan voltammetry under diffusion control, is not completely applicable for predicting peak currents in square-wave voltammetry. This limitation arises from the complex interplay of experimental parameters, such as the square-wave amplitude, potential step, frequency, and temperature, all of which collectively shape the structure of the diffusion layer and the concentration profile of the redox-active species of interest. Unlike linear scan voltammetry, where the concentration gradients evolve in a relatively predictable manner, square-wave voltammetry involves rapid potential modulation that disrupts the classical development of concentration profiles. Consequently, the voltammetric outputs become highly dependent on the dynamic and non-linear interactions between these parameters commonly arise. This makes the application of Randles–Sevcik formalism insufficient to fully describe the behavior of SWV peak currents under diffusional conditions. In practice, the temperature-dependent nature of the diffusion coefficient introduces

additional variability that the Randles–Sevcik framework cannot accommodate. As evidenced in Figures 2 through 6, the peak currents might exhibit a non-trivial dependence on potential step, frequency, temperature, and square-wave amplitude, indicating that no single analytical expression like the Randles–Sevcik equation can universally describe the system. Therefore, a semi-empirical approach remains the most viable strategy to determine which parameters predominantly govern the peak current in SWV, in agreement with the observed experimental trends.

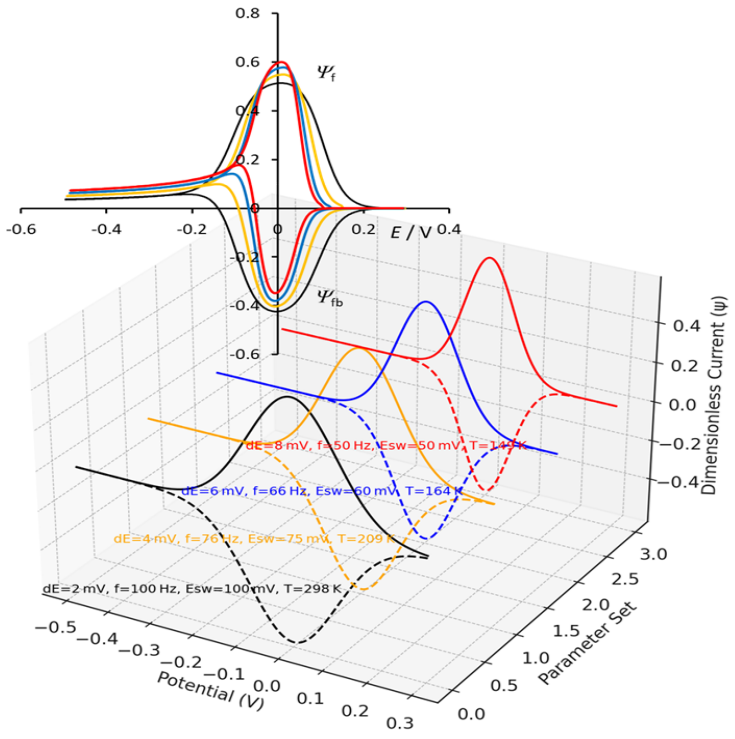

Figure 7. Three-dimensional voltammetric profiles of the forward and backward current components, illustrating their evolution as a function of a unified parameter $\chi/const.$ = 27.528, which incorporates the effects of potential step (dE), frequency (f), square-wave amplitude (E_{sw}), and temperature (T). The parameter χ is defined as $\chi = const.\cdot(F/RT)\cdot[E_{sw}/(dE\cdot f)]^{1/2}$. The combinations of d$E$, f, E_{sw} and T unified in parameter $\chi/const.$ = 27.528 are given in the 3D graph next to each corresponding voltammogram. In the left upper corner, 2D graph of forward and backward current components of voltammograms simulated for $\chi/const.$ = 27.528 corresponding to the conditions given in the 3D plot are shown.

The analysis of square-wave voltammograms presented in Figure 7 reveals a compelling observation: despite the variation of fundamental experimental parameters such as step potential (dE), square-wave amplitude (E_{sw}), frequency (f), and temperature (T), the symmetry and magnitude of the forward and backward current components remain remarkably consistent

when a specific composite parameter is held constant. This dimensionless parameter, defined as $\chi = const. \cdot (F/RT)\cdot[E_{sw}/(dE\cdot f)]^{1/2}$, effectively governs the peak currents of a voltammetric response under Nernstian conditions.

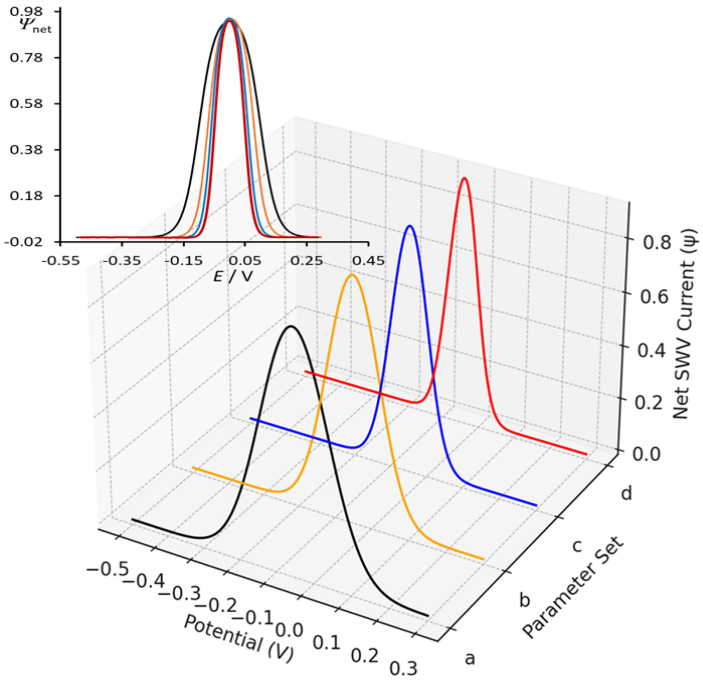

Figure 8. Three-dimensional net square-wave voltammetric profiles corresponding to the voltammetric patterns presented in Figure 7. In the left upper corner, 2-D graph of net SW current components of voltammograms simulated for magnitude of parameter $\chi/const.$ = 27.528 corresponding to the conditions given in the 3-D plot are displayed.

In the last equation, F is the Faraday constant, while R is the universal gas constant. The voltammograms calculated at different sets of (dE, f, E_{sw}, T) but constant χ value (χ/const. = 27.528 in the current set of calculations at Figure 7) exhibit nearly identical ratios between forward and backward peak currents (Figure 7), with net SW peak currents also showing minimal variation (Figure 8). The numerical values of the forward, backward, and net peak currents calculated under varying experimental conditions, specifically different values of step potential, square-wave amplitude, frequency, and temperature, are summarized in Table 1.

Importantly, despite these variations in magnitudes of dE, f, E_{sw}, T, all simulations were performed at a constant value of the composite parameter χ/const. = 27.528. The data presented in Table 1 clearly demonstrate that the χ parameter exerts a significant and consistent influence on the resulting voltammetric peak currents. The near-identical magnitudes of both forward and backward components, as well as the net peak currents across all experimental sets, underscore the critical role of χ in governing the magnitudes of peak currents of theoretical square-wave voltammetric responses.

Table 1. Relevant features of simulated SW voltammograms, calculated at constant parameter χ/const. = $(F/RT)\cdot[E_{sw}/(dE\cdot f)]^{1/2}$ = 27.528. Magnitude of χ/const. = 27.528 is obtained via different combinations of dE, f, E_{sw} and T (magnitudes of peak currents obtained with the tangent method)

Parameter χ /const.= $(F/RT)\cdot[E_{sw}/(dE\cdot f)]^{1/2}$ = 27.528 in all cases, obtained from combination of following simulation parameters	**Magnitude of forward (reduction) peak current $\Psi_{f,p}$**	**Magnitude of backward (oxidation) peak current $\Psi_{b,p}$**	**Magnitude of net SWV peak current $\Psi_{net,p}$**
Black curve: dE = 2 mV, f = 100 Hz, effective scan rate = 200 mV/s E_{sw} = 100 mV, T = 298 K	0.458	-0.457	0.915
Orange curve: dE = 4 mV, f = 76 Hz, effective scan rate = 304 mV/s E_{sw} = 75 mV, T = 209 K	0.460	-0.458	0.918
Blue curve: dE = 6 mV, f = 66 Hz, effective scan rate = 396 mV/s E_{sw} = 60 mV, T = 164 K	0.460	-0.460	0.920
Red curve: dE=8 mV, f = 50 Hz, effective scan rate = 400 mV/s E_{sw} = 50 mV, T = 149 K	0.462	-0.463	0.925

4. CONCLUSION

As shown in previous segments of this work, the Randles–Sevcik equation, traditionally used to describe peak currents dependence in linear scan voltammetry for Nernstian redox systems under diffusion control, is not completely applicable for predicting peak currents in square-wave voltammetry. This limitation arises from the complex interplay of experimental parameters, such as the square-wave amplitude, potential step, frequency, and temperature, all of which collectively shape the structure of the diffusion layer, and so the concentration profile of the redox-active species. Unlike linear scan voltammetry, where the concentration gradients evolve in a relatively predictable manner, square-wave voltammetry involves rapid potential modulation that disrupts the classical development of concentration profiles in diffusion layer. Consequently, the voltammetric outputs become highly dependent on the dynamic and complex interactions between these parameters. This makes the application of Randles-Sevcik formalism insufficient to fully describe the behavior of SWV peak currents under diffusional conditions. Large applied SW amplitudes (larger than 100 mV), and large potential steps (larger than 10 mV) commonly cause huge disruptions of the applied potential. This will generate driving forces that make the redox process to proceed very rapidly. The flattened voltammetric responses and the suppression of well-defined peak formation at large applied SW amplitudes

are attributed to the insufficient development of diffusional concentration gradients within the time frame of the applied potential pulses. These effects highlight the major limitations of applying the Randles–Sevcik formalism under square-wave voltammetric conditions, where the transient and pulsed nature of the technique, coupled with temperature dependences on all voltammetric features, precludes the use of simplified linear diffusion-based models. However, the major results evaluated in this work suggest that a complex parameter χ, defined as $\chi = const.\cdot(F/RT)\cdot[E_{sw}/(dE\cdot f)]^{1/2}$, functions as a key parameter that largely defines the peak currents of SW voltammetric peaks, despite wide variations in input conditions. This behavior holds for E_{sw} in the range of 40 mV and 100 mV, and dE between 2mV and 10 mV, indicating the robustness of parameter χ in defining crucial role across a broad practical domain. This finding opens a new perspective for modeling in square-wave voltammetry and suggests that the χ parameter (which may be referred to as the "*JPG*" parameter, named after the initials of Janeva, Kokoskarova, and Gulaboski) may serve, under SWV conditions, as an analog to the Randles–Sevcik function in linear scan voltammetry. In practice, however, the temperature dependence of the diffusion coefficient introduces additional complexity that falls outside the predictive capacity of the Randles-Sevcik framework. Therefore, this parameter χ reflects a slight dependence of the diffusion coefficient on temperature, consistent with real experiments typically conducted in the range of 285–300 K [20]. Nevertheless, the findings presented in this work may serve as an initial step towards forming a theoretical basis for developing a generalized predictive equation that relates peak currents to measurable parameters under square-wave modulation. Such a parameter-driven approach could significantly facilitate the rational design, interpretation, and standardization of SWV experiments in applied electroanalysis. In our subsequent model, this approach will be applied to identify the governing parameter for square-wave voltammetric peak currents in more complex kinetic systems, as described within the framework of the Butler-Volmer formalism.

Acknowledgments

Rubin Gulaboski thanks the Alexander von Humboldt Foundation (Germany) for the support via project with Ref 3.4-1070534-MKD-IP. All authors of this work would like to thank the "Goce Delcev" University, Stip, Macedonia, for the permanent support.

Declarations of interest

The authors declare no conflict of interest in this reported work.

REFERENCES

[1] F.A. Armstrong, in: A.J. Bard, M. Stratmann, and G.S. Wilson (Eds.), Encyclopedia of Electrochemistry, Wiley-VCH, Weinheim (2020).

[2] J.M. Saveant, and C. Costent, Elements of Molecular and Biomolecular Electrochemistry: An Electrochemical Approach to Electron-Transfer Chemistry, 2nd ed., John Wiley & Sons (2019).
[3] R.G. Compton, and C. E. Banks, Understanding Voltammetry, 2nd ed. Imperial College Press, London, 2011.
[4] N. Elgrashi, K.J. Rountree, B.D. McCarthy, E.S. Rountree, T.T. Eisenhart, and J. L. Dempsey, J. Chem. Educ. 95 (2018) 197.
[5] G.A. Mabbott, J. Chem. Educ. 60 (1983) 697.
[6] P.T. Kissinger, and W.R. Heineman, J. Chem. Educ. 6 (1983) 702.
[7] A. Sevcik, Collect. Czech. Chem. Commun. 13 (1948) 349.
[8] A.J. Bard and R.A. Faulkner, Electrochemical methods: Fundamentals and applications, 2nd ed, Wiley, New York (2011).
[9] V. Mirceski, S. Komorsky-Lovric, and M. Lovric, in: F. Scholz (Ed.), Square-Wave Voltammetry, Theory and Application, Springer, Berlin (2007).
[10] A. Molina, and J. Gonzalez, Pulse voltammetry in physical chemistry and electroanalysis: Theory and applications, F. Scholz, ed. Springer, Germany (2016).
[11] R. Gulaboski, and V. Mirceski, J. Solid State Electrochem. 28 (2024) 1121.
[12] Gamry Instruments. Square-Wave Voltammetry, Gamry Application Notes (2018).
[13] A. Molina, J. Gonzalez, F. Martinez-Ortiz, and R. G. Compton, Geometrical insights of Transient Diffusion Layers, J. Phys. Chem. C 114 (2010) 4093.
[14] J. V. Hernandez Tovar, A. J. Martinez-Garcia, M. Lopez-Tenes, F. Martinez-Ortiz, A. Molina, and J. Gonzalez, Anal. Chem. 97 (2025) 2941.
[15] J.L. Melvile, and R.G. Compton, Electroanalysis 13 (2001) 123.
[16] A. Molina, E. Laborda, F. Martínez-Ortiz, D.F. Bradley, D.J. Schiffrin, and R.G. Compton, J. Electroanal. Chem. 659 (2011) 12.
[17] E. Laborda, J. Gonzalez, and A. Molina, Electrochem. Commun. 43 (2014) 25.
[18] A.A. Sher, A.M. Bond, D.J. Gavaghan, K. Gillow, N.W. Duffy, S. Guo, and J. Zhang, Electroanalysis, 17 (2005) 1450.
[19] R. Gulaboski, M. Lovric, V. Mirceski, I. Bogeski, and M. Hoth, Biophys. Chem. 137 (2008) 49.
[20] R.A. Meyers, Encyclopedia of Physical Science and Technology, 3rd edition (2001) Elsevier.